Sensor Calibration and Registration for Mobile Manipulators

Steven Legowik
Robotic Research, LLC
Gaithersburg, MD , USA
email: legowik@roboticresearch.com

Roger Bostelman[1,2] and Tsai Hong[1]
[1]Intelligent Systems Division
National Institute of Standards and Technology
Gaithersburg, MD, USA
[2]IEM, Le2i, Université de Bourgogne,
Dijon, France
email: roger.bostelman@nist.gov and tsai.hong@nist.gov

***Abstract*—This paper describes the methods used to register a mobile manipulator to a workstation to perform assembly tasks. The nonlinear, least square model of the system is formulated and Ceres Solver is used to compute the position of the robot arm relative to the mobile base. The use of non-contact fiducials to test the accuracy and repeatability of the mobile manipulator positioning in the context of an assembly operation is also discussed. Using mathematical methods and indirect measurements it is possible to compute the offset between physical components of the system where direct measurement is not feasible.**

Keywords- robot; AGV; mobile manipulator; collaborative robotics; registration; Ceres Solver; calibration.

I. INTRODUCTION

Industry is making increasing use of robotics for material transport and processing. These robotic systems make use of many innovative sensing technologies [2]-[5] and control techniques [6]-[9] to improve their versatility and agility. The traditional approach to flexible manufacturing is to use mobile robots to transport materials [10][11] between workstations containing stationary robotic manipulators [6]. Another approach is to move the robotic manipulators between the workstations [12] using an Automatic Ground Vehicle (AGV). This configuration is referred to as a mobile manipulator in this paper. The use of mobile manipulators can be advantageous in a number of situations. It can result in cost savings when a single mobile manipulator can be used to replace several stationary manipulators. The use of mobile manipulators is also useful in cases where the item being worked on is too large to be easily moved. Throughout this paper the term manipulator will refer to the robotic manipulator arm mounted on the mobile base, and the mobile base will be referred to as the AGV. The combination is referred to as a mobile manipulator.

The use of mobile manipulators in manufacturing presents new challenges [6]. The use of intelligent sensing systems such as computer vision or light detection and ranging (LADAR) sensors [13] can be used to measure a workpiece's location and orientation relative to the manipulator. To effectively act on sensor information, the systems need to know precisely where those sensors are located with respect to the other elements of the system. The calibration of a new sensor involves the determination of the position and orientation of the sensor relative to other sensors and manipulators. These parameters are difficult, or even impossible, to measure directly. Sometimes the only way of determining these unobservable system parameters is through the mathematical analysis of the sensor's own data. The calculation of arm-mounted camera offsets using images from the camera has been widely discussed in the literature [14]-[25]. In most of these methods, a key feature is the simultaneous solution of two sets of independent transformations. These transformations are typically the desired offset of the sensor and the pose of a calibration target. The solution of the calibration target pose is typically incidental to the solution of the desired offset. Similar methods can be applied to determining other system offsets.

The focus of this paper is on indirect methods for determining the mounting offset of a robot manipulator on a mobile base. Section II discusses the need to calibrate the offset between the manipulator base and the AGV's coordinate system. It also describes the equipment and methods used to collect the data and evaluate the results of the mounting offset calibration. Section III. discusses two methods of computing the mounting offset: the first using measurements taken at selected positions around a test artifact, and the second a method of computing the offset using Ceres Solver and a selection of measurements from a random set of positions around the test artifact. Section IV. discusses the effectiveness and accuracy of the two calibration methods discussed in Section III. Section V discusses the relative merits of using Ceres Solver for solving this type of calibration problem and the effects of measurement noise on the procedure.

II. WORKSTATION REGISTRATION

This section describes the workstation registration problem, the NIST mobile manipulator testbed, a novel registration artifact, and the use of the artifact for registration.

A. Description of the problem

The goal is to be able to use the AGV to move the manipulator to a workstation and be able to accurately assemble items in that workspace [26]. To perform this task, it is necessary to accurately determine the location of the manipulator relative to the workspace. Two crucial components of this are determining: (1) the actual (not just the commanded) position of the AGV and (2) the position of

 ISBN: 978-1-61208-515-9

the manipulator relative to the AGV. For component one, we need to be able to get the position of the AGV from the navigation system in near real time. All our prior research to this point has involved off-line, AGV position data processing from log files. For the current task, we must be able to pass the position information directly to the computer system that is controlling the manipulator.

The second requirement is to establish the offset between the AGV and the base of the manipulator. This will allow the AGV's position to be used to determine the global location of the manipulator when the AGV stops at a particular work station.

B. NIST Mobile Manipulator Testbed

The mobile manipulator used for the work described in this paper is a part of the National Institute of Standards and Technology (NIST), Robotic Systems for Smart Manufacturing Program. It was assembled as a platform for developing and testing performance standards [26][27] for mobile manipulators in industry.

The mobile manipulator consists of a six-axis manipulator mounted on top of an AGV. The AGV is an electrically-powered, all-wheel drive, automatic forklift designed for material transport in an industrial setting. The AGV navigates from location to location using a path network that is preprogrammed off-line. The AGV location is measured using a navigation system that uses a rotating laser range sensor to detect the locations of reflectors strategically mounted throughout the work area. The positions of the reflectors are surveyed during the initial setup of the system. During operation the position and orientation of the AGV is calculated based on the range and angle to reflectors within range of the navigation sensor.

In order to test the positioning accuracy and repeatability of the mobile manipulator, a laser retro-reflector sensor was mounted as the end-of-arm-tool (EOAT) of the manipulator. A digital signal is output from the sensor when the laser is emitted and reflected to the sensor. The signal is then read by the manipulator controller. Less intense reflections off of other objects in the workstation are ignored. The laser is used to interact with the Reconfigurable Mobile Manipulator Artifact (RMMA) described in the next section.

C. Reconfigurable Mobile Manipulator Artifact

The RMMA [26]-[28] is a test fixture developed at NIST to emulate the environment that would be encountered by a mobile manipulator. It was designed primarily to emulate the positioning requirements of an assembly task, specifically the peg-in-hole insertion task. It does this by providing a set of precisely positioned mount points for reflective targets. The targets are detected using a non-contact, laser retro-reflector sensor designed to detect the presence of retro-reflective targets in line with the laser beam. The sensor is mounted as the EOAT. The targets are designed to determine if the manipulator position is accurate enough for successful peg-in-hole insertion. The RMMA provides a way to test and verify the performance of mobile manipulator systems without the use of expensive 3D tracking systems [29].

The target fiducials are constructed using a piece of reflective material fixed behind a circular aperture. In some of the targets a fixed radius aperture is used, in others a variable aperture is used. A top down view of a target fiducial is shown in Fig. 1. The laser retro-reflector sensor is used to detect the alignment of the manipulator with the fiducial. A signal is returned by the sensor when the laser beam is reflected back by the fiducial. The position accuracy can be adjusted by varying the size of the aperture used to expose the reflector. In addition, a tubular collimator is added to the fiducial to restrict the detection angle of the fiducial. The position of a fiducial can be determined by performing a search starting somewhere near the fiducial's actual position. By performing a spiral grid search with a step size of half the aperture diameter, the position of the fiducial can be determined with an accuracy bounded by the

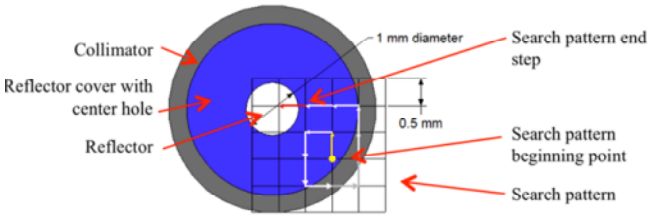

Figure 1. Top down view of an RMMA fiducial showing grid spiral search pattern.

aperture diameter. Fig. 1 illustrates the path followed during a spiral grid search.

Large circular reflectors can also be mounted on the RMMA to aid in mobile manipulator localization. The center of the large reflectors is measured by performing a bisecting search starting from a point within the radius of the reflector. The center is found by searching outward to find the reflector edges and bisecting that chord. After locating the center along one axis, a search for the reflector's edges is performed along an axis perpendicular to the first. After the endpoints of this second chord are determined, the center position of the reflector can be calculated. The bisection search is illustrated in Fig. 2(a). After the centers of two reflectors have been measured, the position and orientation of the pattern can be determined. Then the positions of all the other target reflectors in the pattern can be calculated based on their position relative to the registration reflectors.

 ISBN: 978-1-61208-515-9

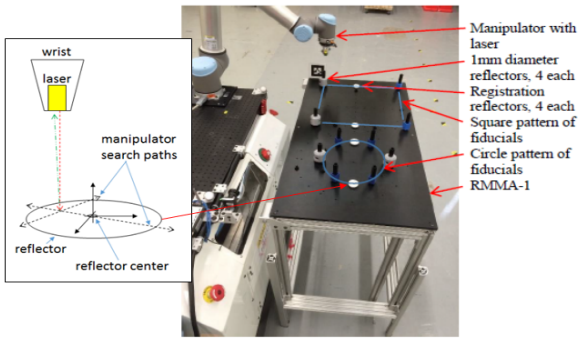

(a) (b)

Figure 2. (a) Bisection search concept, and (b) the mobile manipulator positioned next to the RMMA, the RMMA square and circle patterns, and the large reflectors within each pattern.

D. Registration to RMMA Patterns

The RMMA has a number of precisely-positioned, threaded holes into which the fiducials and reflectors can be mounted to exercise the system. There are two main target configurations: a square target and a circular target as shown in Fig. 2(b). These are used to test the positioning accuracy and repeatability of the mobile manipulator after bisecting the large reflectors.

The two dimensional (2D) pose of the square and circle pattern of small reflectors can be determined by measuring the locations of two reflectors, large or small, on each pattern. The other small reflector locations in the pattern can be calculated based on their relative offsets when given the pattern pose. Either a pair of small reflectors using the search method or a pair of large reflectors using the bisect method can be used to register the mobile manipulator with the workspace represented by each pattern. For example, after moving to the calculated reflector positions, if the small reflector is not immediately detected, a search is performed. The distance between the initial position of the manipulator and the position at the end of the search can be used to provide information on the accuracy of the mobile manipulator's position and the accuracy of the registration.

III. MANIPULATOR CALIBRATION

Calibration of the manipulator onboard the AGV is critical for understanding how to position and orient the manipulator to a workstation. This section describes manual and Ceres Solver methods.

A. Manual calibration method

We experimented with methods to allow strictly manual calibration of the manipulator mounting offset using a number of simple measurements. The idea was to select pairs of calibration data measurements that would lead to the simple calculation of a single value of the manipulator mounting offset. This was done by selecting pairs of positions around the target where the other parameters of the manipulator mounting offset would effectively cancel each other out.

The AGV positions were chosen to cancel out the effects of the other base offset parameters, or to minimize their effect on the computation. In testing, these values were good enough to come up with rough values of the offset, but not good enough for precise positioning of the manipulator. There were some interactions between the calibration variables that could not be completely eliminated using this method. However, the method works well as a sanity check for the other computation methods.

The equations below describe the manipulator offset calibration in a 2D plane. The value being determined is the 2D translational offset and rotation offset of the manipulator relative to the AGV. The reason for doing the calculations in 2D is that the method for taking the measurements using the laser sensor only constrains the position in 2D, and the AGV navigation solution is only 2D.

Fig. 3(a) illustrates a pair of mobile manipulator locations that isolates the x offset of the manipulator base.

$$A_{x1} + O_x - P_{x1} = A_{x2} - O_x + P_{x2}, \quad (1)$$

$$O_x = \tfrac{1}{2} (A_{x2} - A_{x1} + P_{x1} + P_{x2}), \quad (2)$$

where:

P is point in manipulator coordinates (P_x, P_y)

A is AGV coordinate (A_x, A_y, A_a=angle)

O is the manipulator mounting offset (O_x, O_y, O_a=angle)

Fig. 3(b) illustrates a pair of mobile manipulator locations that isolates the y offset of the manipulator base.

$$A_{y1} + O_y - P_{y1} = A_{y2} - O_y + P_{y2}, \quad (3)$$

$$O_y = \tfrac{1}{2} (A_{y2} - A_{y1} + P_{y1} + P_{y2}), \quad (4)$$

Fig. 3(c) illustrates a pair of mobile manipulator locations that isolates the angular offset of the manipulator base.

$$A_{x1} + O_x - P_{x1} + R_1 \sin O_a = A_{x2} + O_x - P_{x2} + R_2 \sin O_a, \quad (5)$$

where

$$R_n = (P_{xn}^2 + P_{yn}^2)^{1/2} \quad (6)$$

and

$$O_a = \sin^{-1}((A_{x1} - A_{x2} - P_{x1} + P_{x2}) / (R_2 - R_1)) . \quad (7)$$

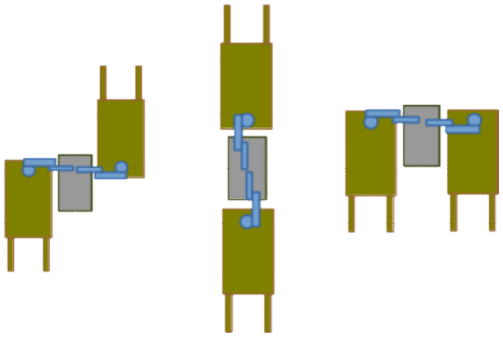

(a) (b) (c)

Figure 3. Mobile manipulator (green) positions relative to the RMMA (gray) selected for manual calibration of manipulator (blue) mounting offset.

These formulas assume the manipulator is mounted on the AGV with its positive y-axis pointing toward the rear

 ISBN: 978-1-61208-515-9

(fork-end) of the AGV (in the direction of the AGV's negative x-axis).

There are a number of issues that limit the effectiveness of this approach for determining the manipulator base location. One issue is that despite the best efforts to position the AGV as described, there will be some errors in alignment. The result is that the other offset terms will not cancel out exactly, and there will be some interaction between the parameters that will affect the results of the calibration.

Another issue with this method is that it does not deal well with measurement error. Each parameter is calculated using a single pair of AGV positions. So any errors in the measurements are reflected directly in the calculated mounting parameters. The effects of measurement noise can be compensated for by averaging together a number of measurements at a given location.

B. Calibration using Ceres Solver

A better way to solve for the manipulator base offset is to express it in terms of a non-linear minimization problem. This allows all the interactions between the base offset parameters and the calibration measurements to be explicitly modeled. After the interactions between the calibration parameters and the calibration data have been modeled, the calibration parameters can be solved using iterative methods. The tool used to compute the iterative solution was the Ceres Solver library [1].

The calibration data consists of paired AGV and manipulator position data taken at various locations around the RMMA. The only constraint on the data is that it needs to be collected at a number of different AGV positions and angles in order for the solver to converge properly. Data from multiple target points can also be used as long as the association is maintained in the data model.

The mobile manipulator system model is formulated as:

$$wp(k) = agvPose(t) * robotPose * rp(k,t), \quad (8)$$

where:

- wp(k) is the estimated position of the *k*th target point in world coordinates;
- agvPose(t) is the measured pose of the AGV in world coordinates at time t;
- robotPose is the estimated pose of the manipulator in AGV vehicle coordinates;
- rp(k,t) is the measured location of the *k*th target point in manipulator coordinates at time t.

The agvPose(t) and robotPose are 2D transformations consisting of a translation and a rotation. The points wp and rp are 2D points. Individual calibration targets are enumerated by *k*, and individual calibration measurements are enumerated by *t*.

The program adjusts the values of wp(k) and robotPose to minimize the residual between the estimated world coordinates of the target points and the position value computed in (8) above using the calibration data. The estimate of the manipulator mounting offset is calculated using the data collected for the manual calibration augmented with additional samples not used in the manual calibration.

The relationship between the calibration data and the free variables is established in Ceres Solver by the creation of *residual blocks*. The residual is defined as the difference between the estimated value of wp and the value of wp calculated by (8). The Ceres Solver then iteratively solves for the values of wp and robotPose that minimize the sum of the squares of all the residuals defined by the residual blocks. Ceres can also make use of a loss function, which can be used to minimize the effect of outliers. When the loss function is $\rho(x) = x$, Ceres minimizes the mean squared error of the residuals. The encapsulation of the residual computation in the residual blocks also allows Ceres to automatically compute the partial derivatives of the modeling equations. This eliminates a potential source of user error.

This problem bears a close similarity to the three-dimensional (3D) simultaneous, robot-world, hand-eye calibration discussed in [14][15][16]. The camera calibration problem is typically expressed as AX = ZB, where X is the 3D pose representing the camera offset and Z is the 3D pose representing the location of the calibration target. It is easy to see that (8) can be manipulated into this form. Both X and Z are unknowns that have to be solved simultaneously. A number of closed-form solutions [14][25] have been proposed to solve for these values. The principle difference between the different solutions is how they resolve the weighting between the positional and rotational components [11] of the residual that defines the 'best' solution to the problem. Given the 2D nature of the current problem, it is probable that a closed-form solution to the problem can be formulated. However, since the calibration parameters do not need to be computed in real time, the iterative solution implemented with Ceres Solver is sufficient. The iterative solution method is also easily adapted to solve for other calibration constants, some of which may not be solvable with a closed-form solution.

More data is generally better data. Unlike the manual calibration approach, the iterative minimization approach can use additional data to minimize the effects of measurement noise. However, care must be taken to provide a suitably rich set of input data. For example, if all the samples were taken at different positions around the workspace, but with the same orientation, it is not possible to determine the orientation offset of the manipulator base. The iterative solution would either not converge, or would converge to an unstable value.

Care must also be taken in the construction of the system model used for iterative minimization. If two or more of the free variables are correlated, the model will be under constrained, and may not be able to converge to an answer. A high degree of correlation between variables can also lead to a high degree of sensitivity to the input data.

IV. RESULTS OF TESTING

The initial set of calibration data was collected manually. The AGV was moved manually to various locations around the RMMA and its position was recorded. Then the

 ISBN: 978-1-61208-515-9

manipulator was moved manually to the positions of the first and second reflectors of the square target. The manipulator was moved until the retro-reflector sensor detected the reflectors. Then the position of the manipulator was manually recorded.

The reflectors used to collect the calibration data had a 3.2 mm (1/8 in) aperture. The positions of the AGV relative to the RMMA for the manual data collection are shown in Fig. 4. A subset of these measurements, shown in Fig. 3, was used to perform the manual calibration described in Section III.A. The orientation of the EOAT was maintained constant relative to the manipulator base so that any lateral offset of the sensor from the tool center could be ignored. Any offset at the tool becomes part of the base offset for the purposes of this calibration. A subsequent calibration of the base offset using all of the collected data was performed using Ceres Solver.

Testing of the manipulator base calibration was performed using an automated test program and the RMMA. A program was set up to drive the AGV to ten different positions around the RMMA as shown in Fig. 5. At each docking location, the position of the AGV, the world coordinate of the reflector, and the manipulator base offset were used to compute the robot coordinates of the reflectors using (8). After positioning the sensor, a search was performed to determine how far off the position calculation was.

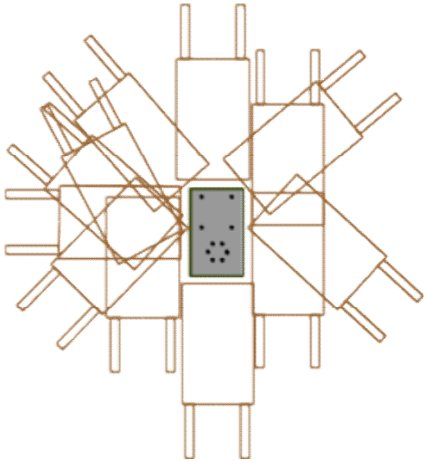

Figure 4. Position and orientation of AGV relative to the RMMA from manually collected calibration data.

Ideally, it should be possible to move the manipulator directly to the reflector based on the position of the AGV. Unfortunately, noise and systematic errors in the AGV position data prevent this. Fig. 6 shows a plot of consecutive samples of the AGV's *x*-axis position as the AGV sits motionless. The graph also shows a plot of the average value of samples 1 through n. This shows roughly how many samples need to average together to produce a reasonably stable position value. The *y* position and the orientation angle exhibit similar noise. The AGV position data is available at about 16 Hz, so it requires about 6.25 seconds to collect 100 samples. In this 2D case a simple average of the orientation angles is sufficient. In the general case of 3D orientations, greater care needs to be observed in averaging the orientation [32][33]. In addition to the random noise, tests also indicate that there are some systematic biases in the AGV position data depending on the location of the AGV.

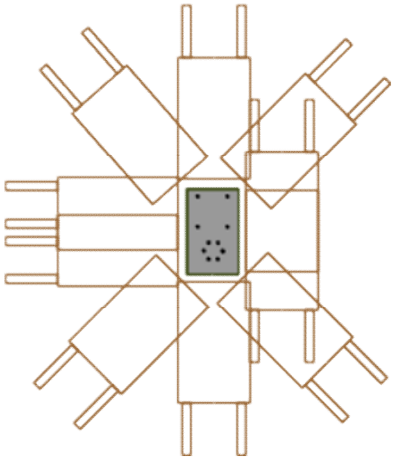

Figure 5. Docking locations used for automated data collection and system evaluation.

The goal is to be able to align the manipulator with the workspace in the minimum amount of time. The ideal situation is to be able to perform the insertion task immediately on arrival at the workstation. However, in this case it is necessary to compensate for the unavoidable measurement errors. It becomes a tradeoff between time spent averaging the position data to produce a stable value vs. time spent searching for registration points in the workspace.

The manual calibration method described in section III.A generated a base offset of (x = 831.5, y = - 7.5) mm and a rotation of 90.6°, yielding a mean square error of 1.25 mm and a maximum residual of 6.3 mm. The Ceres Solver came up with an offset of (x =833.637, y = -8.22223) mm and a rotation of 90.5314°, yielding a mean square error of 1.19 mm and a maximum residual of 10.7 mm. The Ceres Solver was seeded with a variety of initial conditions, including setting all the variable parameters to 0, and had no problems with convergence. The resulting offset positions agreed with each other within 0.1 mm

V. CONCLUSIONS

With care, Ceres Solver has proven to be a valuable tool in calibrating a variety of hard to measure constants in our robotic systems. It provides an easy to use framework for solving difficult non-linear problems iteratively. The main issues that have to be observed are that the model cannot be either over or under constrained if Ceres Solver is to converge properly.

 ISBN: 978-1-61208-515-9

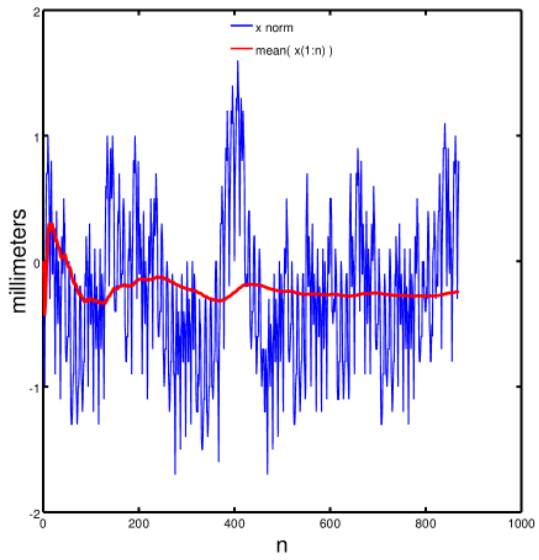

Figure 6. (blue)AGV position along x-axis, normalized to the first sample, x(1); (red) the mean of the normalized x value from x(1) to x(n).

Using Ceres Solver, we were able to compute the base offset of the manipulator mounted on a mobile platform despite the fact that the location of the AGV origin was not directly measureable. Using the computed offset and the location of the AGV, we were able to position the manipulator end effector within a few millimeters of the target regardless of the position and orientation of the AGV. While perfect initial positioning was not possible, the search time required to achieve the desired alignment accuracy was greatly reduced by improving the initial positioning of the manipulator.

The limiting factors in being able to accurately position the end effector are the noise and systematic errors in the AGV navigation sensor. This affects both the final position calculation and the accuracy of the manipulator base transform. The AGV position errors in the measurement used to compute the base offset affect the quality of the solution derived. The quality of the solution can be assessed by examining the residuals left after the model has converged to a solution for the free parameters. Large residuals indicate corresponding errors in the calibration data, either random or systematic.

We plan on pursuing other methods to increase the speed of the workspace registration. The spiral grid search increases in time proportional to the square of the initial error. Performing a bisecting search on the large reflectors goes up approximately linearly with the size of the maximum expected error, since the size of the reflector needs to be scaled up to encompass the maximum initial positioning error. In the future, we are planning to investigate the use of camera-based position estimates to improve the alignment time.

DISCLAIMER

Commercial equipment, software, and materials are identified in order to adequately specify certain procedures. In no case does such identification imply recommendation or endorsement by the National Institute of Standards and Technology, nor does it imply that the materials, equipment, or software are necessarily the best available for the purpose.

REFERENCES

[1] S. Agarwal and K. Mierle, “Ceres solver,” http://ceres-solver.org [retrieved August, 2016].

[2] B. Hamner, S. Koterba, J. Shi, R. Simmons, and S. Singh, “Mobile robotic dynamic tracking for assembly tasks,” IEEE/RSJ International Conference on Intelligent Robots and Systems, pp. 2489-2495, 2009.

[3] R. Bostelman, T. Hong, and G. Cheok, "Navigation Performance Evaluation for Automated Guided Vehicle," 2015 IEEE International Conference on Technologies for Practical Robot Applications (TePRA), pp. 1-6 , 2015.

[4] R. E. Mandapat, “Development and evaluation of positioning systems for autonomous vehicle navigation,” Florida University Gainesville Center for Intelligent Machines and Robotics, pp. 1-277, 2001.

[5] A. Kelly, B. Nagy, D. Stager, and R. Unnikrishnan, "Field and service applications an infrastructure free automated guided vehicle based on computer vision an effort to make an industrial robot vehicle that can operate without supporting infrastructure." IEEE Robotics & Automation Magazine, pp.24-34, 2007.

[6] B. Hamner, S. Koterba, J. Shi, R. Simmons, and S. Singh, “An autonomous mobile manipulator for assembly tasks,” Autonomous Robot, pp.131-149 , 2010.

[7] J. Vannoy and J. Xiao, “Real-time Adaptive Motion Planning (RAMP) of mobile manipulators in dynamic environments with unforeseen changes,” in IEEE Trans. on Robotics, pp.1199-1212 , 2008.

[8] H. Martínez-Barberá and D. Herrero-Pérez, "Autonomous navigation of an automated guided vehicle in industrial environments." Robotics and Computer-Integrated Manufacturing, pp.296-311, 2010.

[9] R. C. Arkin and R. Murphy, "Autonomous navigation in a manufacturing environment," IEEE Transactions on Robotics and Automation, pp.445-454 ,1990.

[10] H. F. Durrant-Whyte, "An autonomous guided vehicle for cargo handling applications." The International Journal of Robotics Research, pp.407-440, 1996.

[11] H. Martínez-Barberá and D. Herrero-Pérez, "Autonomous navigation of an automated guided vehicle in industrial environments." Robotics and Computer-Integrated Manufacturing, pp.407-440, 2010.

[12] S. Bøgh, M. Hvilshøj, M. Kristiansen, and O. Madsen, "Autonomous industrial mobile manipulation (AIMM): from research to industry." In 42nd International Symposium on Robotics. Pp. 1-9, 2011.

[13] M. Hvilshøj and S. Bøgh, “Little Helper-An autonomous industrial mobile manipulator concept,” International Journal of Advanced Robotic Systems, pp.80-90, 2011.

[14] M. Shah, “Solving the Robot-World/Hand-Eye Calibration Problem Using the Kronecker Product,” ASME Journal of Mechanisms and Robotics, Vol. 5, 031007, pp. 1-7, 2013.

[15] F. Dornaika and R. Horaud, “Simultaneous robot-world and hand-eye calibration, “IEEE Transactions on Robotics and Automation, pp.617-622 ,1998.

[16] H. Zhuang, Z. Roth, and R. Sudhakar, “Simultaneous robot/world and tool/flange calibration by solving

 ISBN: 978-1-61208-515-9

homogeneous transformation of the form AX = YB," IEEE Trans. Robot. Automat, pp.549-554, 1994.

[17] A. Geiger, F. Moosmann, O. Car, and B. Schuster, "Automatic calibration of range and camera sensors using a single shot," ICRA, pp. 3936-3943, 2012.

[18] H. S. Alismail, D. Baker, and B. Browning, "Automatic calibration of a range sensor and camera system," Second International Conference on 3D Imaging, Modeling, Processing, Visualization & Transmission. IEEE, pp. 286-292 ,2012.

[19] Z. Zhang, "A flexible new technique for camera calibration," IEEE Transactions on pattern analysis and machine intelligence, pp.1330-1334, 2000.

[20] J-Y. Bouguet, "Camera calibration toolbox for matlab," < http://www.vision.caltech.edu/bouguetj/calib_doc/> [retrieved August, 2016].

[21] J. Weng, P. Cohen, and M. Herniou. "Camera calibration with distortion models and accuracy evaluation," IEEE Transactions on pattern analysis and machine intelligence 14.10, pp.965-980, 1992.

[22] O. D. Faugeras, Q.-T. Luong, and S. J. Maybank, "Camera self-calibration: Theory and experiments," European conference on computer vision, Springer Berlin Heidelberg, pp. 321-334, 1992.

[23] Y. Huang, X. Qian, and S. Chen, "Multi-sensor calibration through iterative registration and fusion, " Computer-Aided Design, pp.240-255, 2009.

[24] S. Spiess, V. Vincze, and M. Ayromlou, "On the calibration of a 6D laser tracking system for contactless, dynamic robot measurements," Instrumentation and Measurement Technology Conference, pp. 1203-1208 ,1997.

[25] M. Shah, R. D. Eastman, and T. Hong, "An overview of robot-sensor calibration methods for evaluation of perception systems," In Proceedings of the Workshop on Performance Metrics for Intelligent Systems, pp. 15-20, ACM, 2012.

[26] R. Bostelman, T. Hong, and J. Marvel, "Performance Measurement of Mobile Manipulators", SPIE 2015, Baltimore, MD, Vol. 9498, pp. 1-9, April 2015.

[27] R. Bostelman, T. Hong, and S. Legowik, "Mobile Robot and Mobile Manipulator Research Towards ASTM Standards Development", SPIE 2016, Baltimore, MD, pp. 98720F-98720F , 2016.

[28] R. Bostelman, S. Foufou, S. Legowik, and T. Hong "Mobile Manipulator Performance Measurement Towards Manufacturing Assembly Tasks", 13th IFIP International Conference on Product Lifecycle Management (PLM16), Columbia, SC, July 11-13, Vol. 9892, pp. F1-F10, 2016.

[29] R. Bostelman, J. Falco, M. Shah, and T. Hong, "Dynamic Metrology Performance Measurement of a Six Degree-of-Freedom Tracking System Used in Smart Manufacturing", Autonomous Industrial Vehicles: From the Laboratory to the Factory Floor, ASTM Book chapter 7, 2016.

[30] R. Bostelman, R. Eastman, T. Hong, O. A. Enein, S. Legowik, and S. Foufou, "Comparison of Registration Methods for Mobile Manipulators," CLAWAR, 2016.

[31] M. Shah, "Comparing Two Sets of Corresponding Six Degree of Freedom Data," Computer Vision and Image Understanding, Volume 115, Issue 10, pp. 1355-1362. 2011.

[32] R. Hartley, J. Trumpf, Y. Dai, and H. Li, "Rotation averaging," International journal of computer vision, 103(3), pp.267-305, 2013.

[33] F. L. Markley, Y. Cheng, J. L. Crassidis, and Y. Oshman, "Averaging quaternions," Journal of Guidance, Control, and Dynamics, pp.1193-1197, 2007.

 ISBN: 978-1-61208-515-9